Journal of Electrical and Electronic Engineering
2017; 5(2): 53-62
http://www.sciencepublishinggroup.com/j/jeee
doi: 10.11648/j.jeee.20170502.15
ISSN: 2329-1613 (Print); ISSN: 2329-1605 (Online)

Control Strategy for Distributed Integration of Photovoltaic and Energy Storage and Wind Power Systems in DC Micro-Grid

Sherku Panjei

Electrical Engineering, Qazvin Branch, Islamic Azad University, Qazvin, Iran

Email address:
Sh.panjei@qiau.ac.ir

To cite this article:
Sherku Panjei. Control Strategy for Distributed Integration of Photovoltaic and Energy Storage and Wind Power Systems in DC Micro-Grid. *Journal of Electrical and Electronic Engineering.* Vol. 5, No. 2, 2017, pp. 53-62. doi: 10.11648/j.jeee.20170502.15

Received: March 3, 2017; **Accepted**: March 16, 2017; **Published**: April 7, 2017

Abstract: Small DC networks to communicate effectively with a variety of output sources such as photovoltaic systems and wind energy storage systems,. If in addition the system DC power is fed over the need to transform and rectify AC network resources compared with a small decrease. Use most of the renewable energy the different factors fine network operates independently suggestions have been. When the system is network -independent, and the exploitation of natural and production of active power by a converter AC balance will be funded constant DC voltage is guaranteed Successful performance of the system in different positions by a coordinated strategy on energy storage systems and photovoltaic systems and wind energy will be discussed And about time management including load and battery state is considering proposals have been Differences by network performance monitoring method is specified MATLAB / SIMULINK, simulation proved strong on performance and determining the status of various systems and control function is proposed.

Keywords: Photovoltaic Systems, Battery Energy Storage Systems, Wind Power, Micro-Grid Dc, Renewable Energy

1. Introduction

Renewable energy conversion systems, low voltage AC distribution systems as generators or micro-grid AC distribution with respect to environmental issues is considered more. When the system is network – independent, and the exploitation of natural and production of active power by a converter AC balance will be funded constant DC voltage is guaranteed. Cost and system that can eliminate the DC-AC or AC-DC power conversion stages required in AC micro-grids for the integration of mentioned renewable energy sources and loads. This paper presents a new synchronous-reference-frame (SRF)-based control method to compensate power-quality (PQ) problems through a three - phase four- wire unified PQ conditioner (UPQC) under unbalanced and distorted load conditions. The proposed UPQC system can improve the power quality at the point of common coupling on power distribution systems under unbalanced and distorted load conditions. The simulation results based on MATLAB/SIMULINK are discussed in detail to support the SRF-based control method presented in this paper. The Proposed approach is also validated through experimental study with the UPQC hardware prototype [1]. This paper presents the modeling and simulation of a high-speed single-shift micro turbine generation system this unit has four parts: a compressor-turbine, a permanent magnet generator, a three phase's bridge rectifier and inverter. The model is built from the dynamics of each part with their interconnections, and two different control strategies suitable respectively for isolated and grid connected operation were developed. Finally simulation studies have been carried out under a stepped load. The model is developed in the MATLAB/Simulink (Matlab2007a) and implemented in power system toolboxes. This model is a useful tool for studying the various operational aspects of micro turbines [2]. This paper presents an advanced control strategy for the rotor and grid side converters of the doubly fed induction generator (DFIG) based wind turbine (WT) to enhance the low-voltage ride-through (LVRT) capability according to the grid connection requirement. Within the new control strategy, the rotor side controller can convert the imbalanced power into the kinetic energy of the WT by increasing its rotor

speed, when a low voltage due to a grid fault occurs at, e.g., the point of common coupling (PCC). The proposed grid side control scheme introduces a compensation term reflecting the instantaneous DC-link current of the rotor side converter in order to smooth the DC-link voltage fluctuations during the grid fault. A major difference from other methods is that the proposed control strategy can absorb the additional kinetic energy during the fault conditions, and significantly reduce the oscillations in the stator and rotor currents and the DC bus voltage. The effectiveness of the proposed control strategy has been demonstrated through various simulation cases. Compared with conventional crowbar protection, the proposed control method can not only improve the LVRT capability of the DFIG WT, but also help maintaining continuous active and reactive power control of the DFIG during the grid faults [3].

This paper two alternative modes of operation for the current-source fly back inverter are investigated in this paper. The discontinuous conduction mode (DCM), where a constant switching frequency (CSF) control method is applied, and the boundary between continuous and DCM (BCM) that is introduced for photovoltaic (PV) applications in this paper (where a variable switching frequency control method is applied). These two control methods are analytically studied and compared in order to establish their advantages as well as their suitability for the development of an inverter for decentralized grid-connected PV applications. An optimum design methodology is developed, aiming for an inverter with the smallest possible volume for the maximum power transfer to the public grid and wide PV energy exploitation. The main advantages of the current-source fly back inverter are very high-power density and high efficiency due to its simple structure, as well as high-power factor regulation. The design and control methodology are validated by personal computer simulation program with integrated circuit emphasis (PSPICE) simulation and experimental results, accomplished on a laboratory prototype [4].

This paper introduces a new control strategy for battery energy storage systems used in wind generation. It is specifically targeted to large wind installations, specifically offshore wind applications. This control strategy maximizes the life of the battery and increases the efficiency of the energy storage system while still balancing the power fluctuations of a large wind turbine system. The depth of discharge and remaining battery life are the key parameters considered in this approach. The proposed control scheme is applied to the battery package such that each battery cell is controlled individually. Individual cell depth of discharge is controlled and cell life is calculated periodically so that all cells within the package reach the end of life at the same. Total storage capacity and individual battery cell size are calculated based on the characteristics of the wind turbine. To verify the presented method, a case is studied in PSCAD and corresponding results are provided [5].

This paper the amount of non-scheduled small scale distributed generation (DG) units are increasing, lack of fault ride through (FRT) capability of these generators may have an adverse effect on the overall power system. This study focuses on the basics of transient overvoltage issue arising under faulty condition with integration of power-electronic (PE) interface based DG units in a system. Reasons behind this overvoltage issue and its impact on DG integration with present grid standard have been investigated. A methodology has been utilized to overcome this overvoltage issue in a system, which has conventional generator as well as wide penetration of full-converter based solar and wind generation. An IEEE industrial test system with varieties of motor loads has been used to carry out the analysis and to verify the methodology [6].

This paper presents a new control method based on synchronous reference frame (SRF) to offset the problems of power quality (PQ) through a mechanism of PQ (UPFC) integrated 4-wire, 3phase conditions Reload uneven and irregular deals The proposed system is capable of UPFC power quality at the point of coupling Subscribe to the distribution system can be improved in terms of load imbalance and irregular Details of the results of the simulations performed in MATAB / Simulink to verify SRF based control method is presented in this paper have been discussed he proposed approach through in vitro study with the prototype hardware is UPQC for validation [7].

This paper proposes a Z-source inverter system for a split-phase grid-connected photovoltaic system. The operation principle, control method and characteristics of the system are presented a comparison between the new and traditional system configurations is performed. Simulation and experimental results are also shown to verify the proposed circuit and analysis [8].

This paper presents a half-bridge single-phase two-wire (1phi2W) photovoltaic (PV) inverter system that can perform both active power filtering and real power injection. In the proposed system, it needs only two active switches, reducing cost significantly. In addition, output current of the inverter can be controlled to prevent switches from exceeding their current ratings. Thus, power rating of the inverter can be effectively used and power quality can be improved. For controlling inverter output current, an amplitude-clamping algorithm and an amplitude-scaling algorithm are proposed, which can determine inverter current command without needs of complicated calculation. Simulations and experimental results have verified the feasibility of the proposed PV inverter system and the two current control algorithms [9].

2. DC Micro-Grid Structure and Circuit Configuration

The investigated DC micro-grid layout is shown in Fig. 1. The system consists of a PV source connected through a DC/DC boost converter and a wind power and a battery energy storage, which is connected through a bi-directional buck-boost DC/DC converter. The BESS is utilized to balance the power difference between the PV power supply

and load demand in islanding mode. A bi-directional DC/AC converter called GS-VSC is also used to connect the DC bus and AC main grid, which enables bi-directional power flow. PV and BESS are at different location in the system therefore a decentralized control strategy based on MDBS is considered for the coordination of PV and BESS and wind power in the system. The primary source of power generation for the DC micro-grid is the PV system, which is controlled to operate at MPPT. The battery meets the sensitive load demand to maintain a continuous supply of power in case of fluctuations in the main grid or during islanding operation.

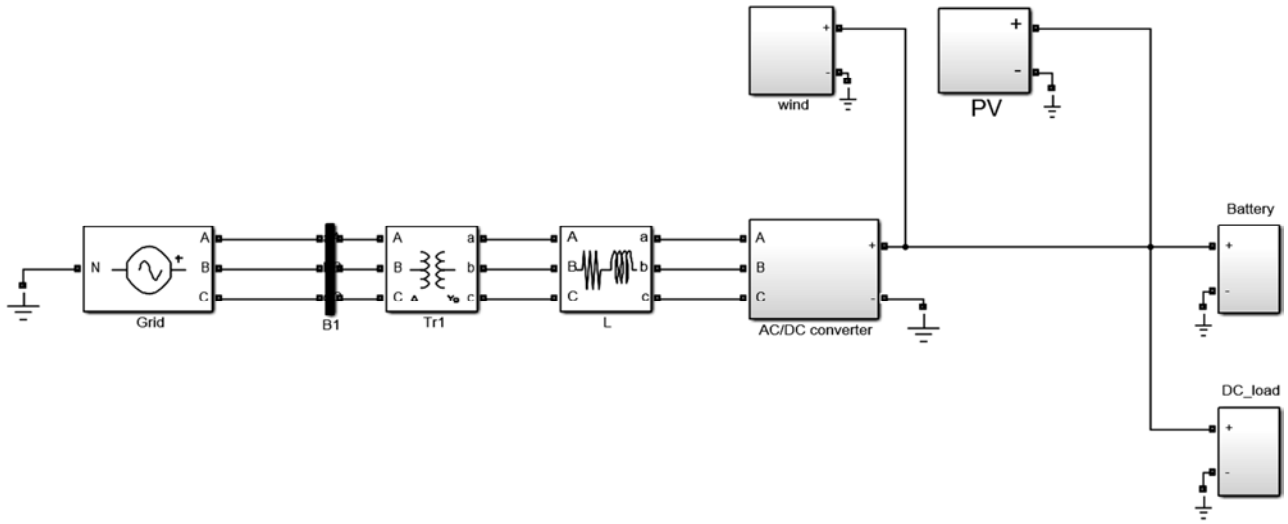

Figure 1. *The layout of the studied DC micro-grid for the integration of PV and wind power and BESS.*

3. Squirrel Cage Induction Generator with Full Power Converter

The system which it is treated can be seen in Fig. 2. The SCIG is attached to the wind turbine by means of a gear box. The SCIG stator windings are connected to a full power converter (back to back).

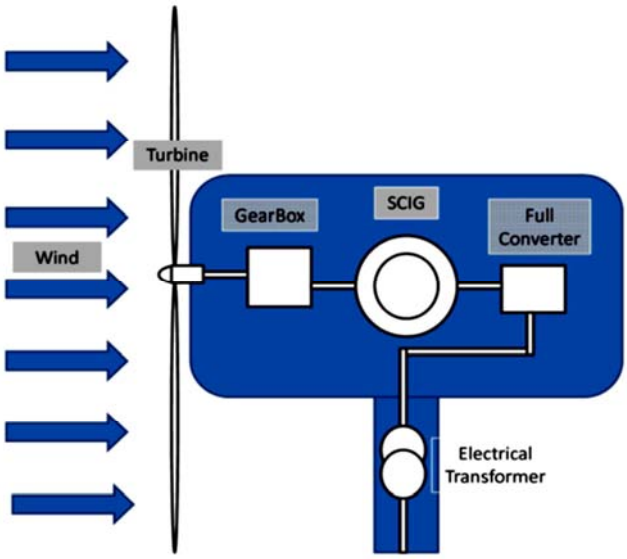

Figure 2. *General System Scheme.*

The wind turbine is the responsible for transforming wind power into kinetic energy. Use full power can be determined using the following equation:

$$P_{wind} = \frac{1}{2}.C_p.\rho.A.v_W^3 \quad (1)$$

Linkage fluxes can be written as:

$$\begin{Bmatrix} \lambda sq \\ \lambda sd \\ \lambda rq \\ \lambda rd \end{Bmatrix} = \begin{bmatrix} Ls & 0 & M & 0 \\ 0 & Ls & 0 & M \\ M & 0 & Lr & 0 \\ 0 & M & 0 & Lr \end{bmatrix} \begin{Bmatrix} isq \\ isd \\ irq \\ ird \end{Bmatrix} \quad (2)$$

The torque can be expressed as:

$$Tm = \frac{3}{2}P.M(i_{sq}i_{rd} - i_{sd}i_{rq}) \quad (3)$$

The active and reactive power yields:

$$Ps = \frac{3}{2}(v_{sq}i_{sq} + v_{sd}i_{sd}) \quad (4)$$

$$Qs = \frac{3}{2}(v_{sq}i_{sd} - v_{sd}i_{sq}) \quad (5)$$

4. System Modeling and Control

4.1. Modeling of PV System

4.1.1. PV Array Modeling

Since the PV characteristics can significantly influence the design and operation of power converter and the control system, a brief review of PV array modeling is presented in this section. Different equivalent circuits of a PV cell have been proposed in the literature. The single-diode circuit is the most commonly used model Fig. 6 shows the single-diode equivalent circuit of a PV cell. The circuit is composed of a current source, a diode in parallel with the current source, the series resistance, and the parallel resistance [10].

$$I_{PV}(V_{PV}) = I_g - I_d - \left(\frac{V_{PV}+R_S I_{PV}}{R_P}\right) \quad (6)$$

$$I_d = I_O\left(e^{\frac{q(V_{pv}+R_S I)}{MskTa}} - 1\right) \quad (7)$$

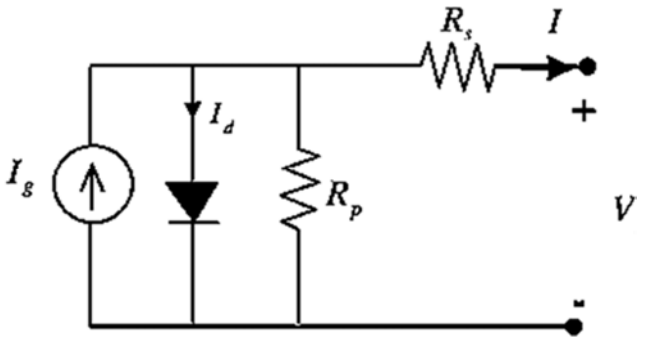

Figure 3. *Single-diode equivalent circuit of a real PV module.*

The current source I_g modeling the photon-generated electron - whole pairs under the influence of the built-in field and is a function of the pen junction temperature (T) and Solar radiation. Norton equivalent circuit is exploited to model a PV array including N_P parallel and Ns series connected PV cells. The circuit consists of the equivalent current source (I_{array}) and the equivalent resistance (R_{array}) defined as:

$$Iarray = N_p I \frac{RP}{R_p+R_s} \quad (8)$$

$$Rarray = \frac{NS}{NP}(R_P + R_S) \quad (9)$$

4.1.2. PV System AND Its Control Algorithm

A boost DC/DC converter is exploited to connect the PV array to the micro-grid. The circuit diagram of the PV system is shown in Fig. 5. MPPT algorithm has two basic assumptions 1. IV characteristic should have identical modules PV 2. Temperature and sun exposure is the same for both modules. For small size PV modules which are considered in this study, these assumptions are accepted at the maximum power point of the module PV. Module increasing resistance equals with its DC resistance. Therefore at each working point through monitoring it will be determined whether current power point is located at the right or the left of the MPP. in The parallel operation of two modules the slope of the curve can easily be calculated from the difference between the voltage and current modules. Fig. 8. Shows Flowchart of MPPT algorithm to track the maximum.

Power point. MPPT algorithm can be easily implemented and there are no need to memory and measuring devices, so the need for comparing the current and previous points will be eliminated. Furthermore in this method no oscillation of working point is observable at any time. Since the controller with through monitoring tracks the maximum power point.

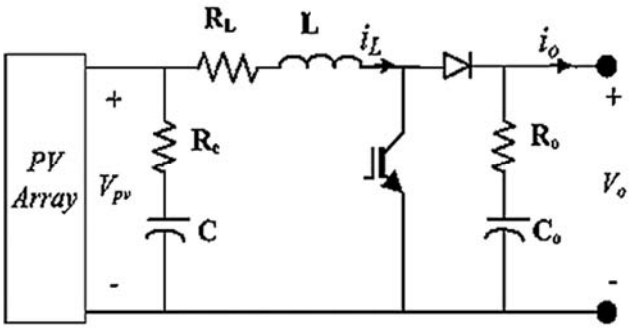

Figure 4. *Boost converter for the PV system.*

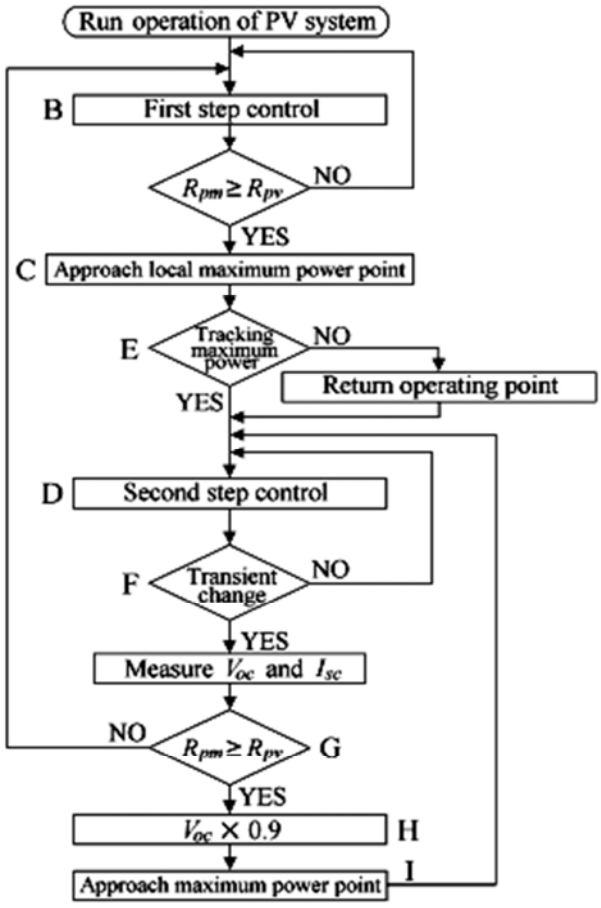

Figure 5. *Control strategy of maximum power point.*

4.1.3. Small Signal Modeling of PV System

Due to nonlinear characteristic of PV array, a linear PV model is necessary for the small signal analysis and controller design. The I -V curve of a typical photovoltaic output is shown in Fig. 6. The derivative of the nonlinear model of PV at a given (V, I) point can be:

$$g(V,I) = \frac{\delta ipv}{\delta vpv}\Big|_{(V,I)} = \frac{A_0+1/R_p}{1+R_S/R_p+R_S A_0} \quad (10)$$

$$A_0 = I_0\left(\frac{qe^{\frac{q(v+RsI)}{MskTa}}}{MskTa}\right) \quad (11)$$

The PV model can be rewritten as:

$$i_{pv}(t) = g(V,I)vpv(t) \quad (12)$$

Linearizing Equation (20) using Perturbation and Linearization method leads to the following linearized model of PV.

$$i_{pv} + i'_{pv} = g(V,I)(Vpv + V'pv) \quad (19)$$

$$v'^{pv} = V_{pv}^{eq} - R_{pv}^{eq} i'pv \quad (20)$$

$$V_{pv}^{eq} = -Vpv + \frac{Ipv}{g} \quad (21)$$

$$R_{pv}^{eq} = -\frac{1}{g} \quad (22)$$

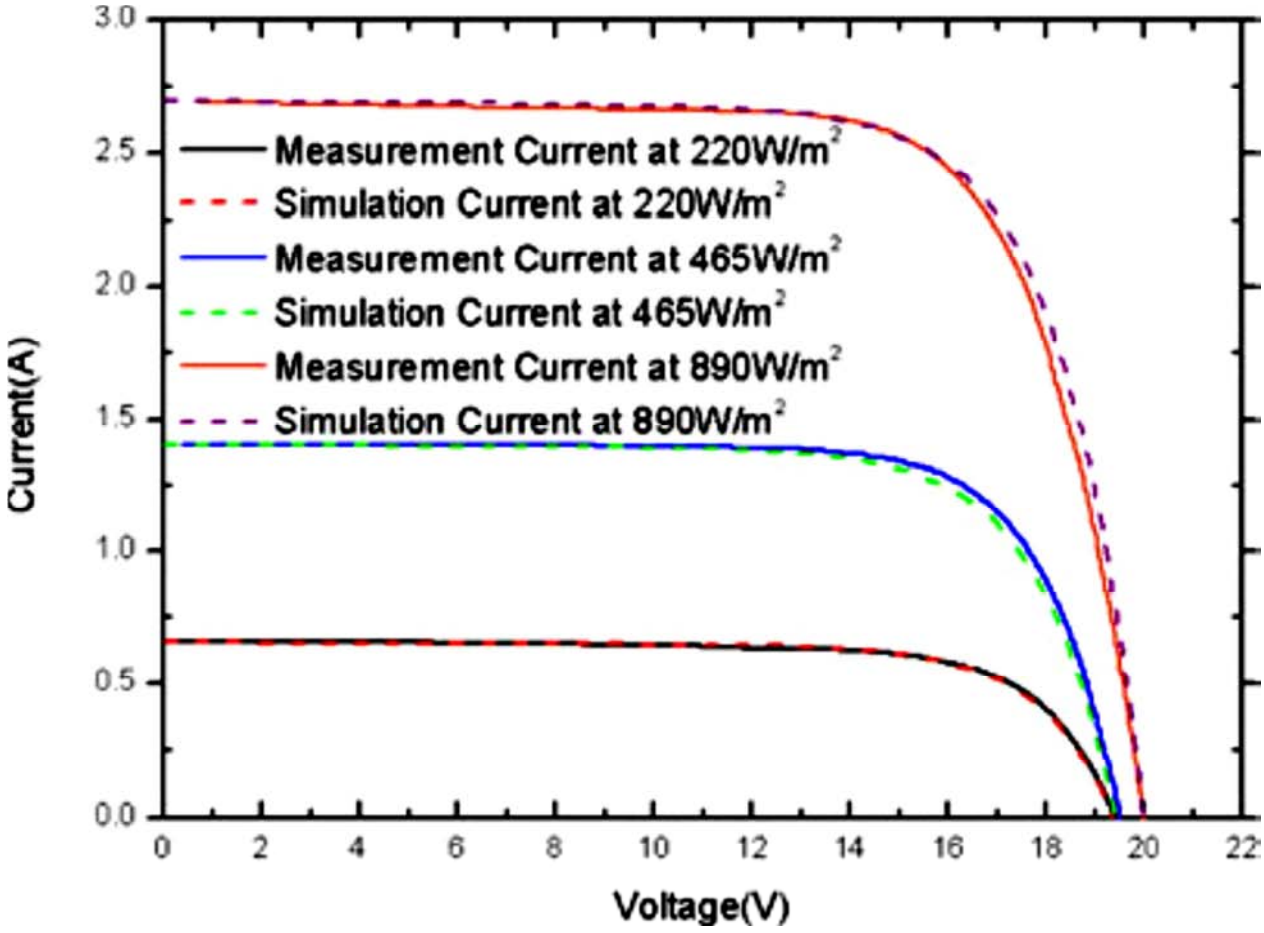

Figure 6. *Linear approximation of photovoltaic output characteristics.*

$$\frac{dil}{dt} = -\frac{R_L}{L} iL + \left(\frac{1-d}{L}\right) vo + \frac{1}{L} vpv \quad (13)$$

$$\frac{dvc}{dt} = \left(\frac{1-d}{C}\right) iL - \frac{1}{C} io \quad (14)$$

$$vpv = RcC\frac{dvc}{dt} + vc \quad (15)$$

$$\frac{dvo}{dt} = \left(\frac{1-d}{C}\right) iL - \frac{1}{C} io \quad (16)$$

The boost converter is intended to control the PV voltage in order to track the MPP and to regulate the DC voltage in the voltage control mode. A small signal model of the PV system with peak current-mode along with input voltage controlled boost converter can now be constructed by perturbation and linearization of Equations (24)- (28) as follows:

$$\frac{v'pv}{i'L} = -\frac{R_{pv}^{eq}(1+RcCs)}{1+\left(R_{pv}^{eq}+Rc\right)Cs} \quad (17)$$

$$iL'd' = Vo\frac{1+\left(R_{pv}^{eq}+Rc\right)Cs}{s2+\frac{\left(R_{pv}^{eq}RcC+RL\left(R_{pv}^{eq}+Rc\right)+L\right.}{\left(LC\left(R_{pv}^{eq}+Rc\right)\right)}S+\frac{\left(R_{pv}^{eq}+RL\right)}{\left(LC\left(R_{pv}^{eq}+Rc\right)\right)}} \quad (18)$$

4.2. Modeling of BESS

4.2.1. Battery Modeling

Due to the nonlinear characteristic of battery, its proper representation in the controller becomes another challenge. Different models for battery behavior simulation with different degrees of complexity and simulation behavior are available. The simplest and commonly used model of a battery contains an ideal voltage source in series with a constant internal resistance. The equivalent circuit model is depicted in Fig. 10 and can be described by the following equations,

$$\mathrm{V_{batt}} = \mathrm{Eg} - \mathrm{i_{batt}R_{batt}} \quad (23)$$

$$\mathrm{E_g} = \mathrm{E_{g0}} - \mathrm{k}\frac{\mathrm{Q}}{\mathrm{Q}-\int \mathrm{i_{batt}dt}} + \mathrm{Aexp(B.}\int \mathrm{i_{batt}dt} \quad (24)$$

The voltage source Eg represents the voltage at open circuit between the battery terminals and depends directly on the stored energy. The state of charge of the battery can also be described by the following equations,

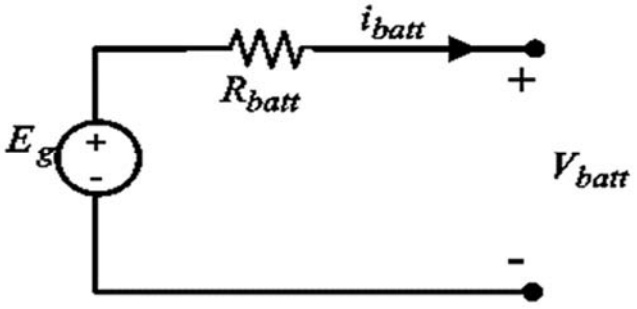

Figure 7. *Equivalent circuit for the battery.*

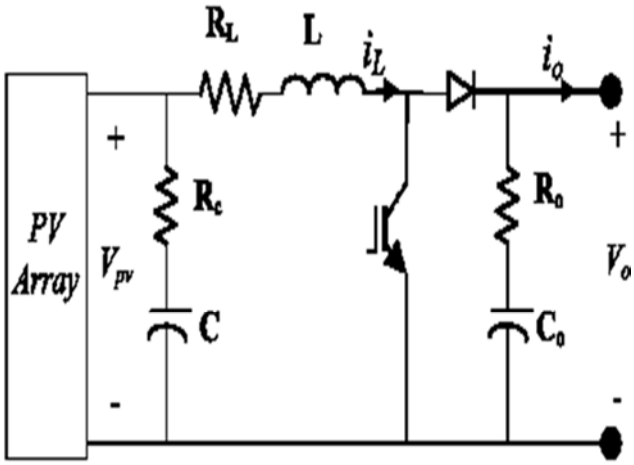

Figure 8. *Bi-directional buck-boost battery converter.*

$$\mathrm{SoC(ti)} = \frac{1}{\mathrm{Q(ti)}}\int_{\infty}^{\mathrm{ti}} \eta_c(t) I_{batt}(t)dt \quad (25)$$

$$Q(ti) = \frac{C_{nominal} c_{t\,coef}}{1+Acap(\frac{|I_{batt}(t)|}{I_{nominal}})^{Bcap}}\left(1 + \alpha c \Delta T(t) \beta c \Delta T^2(t)\right) \quad (26)$$

$$I_{nominal} = \frac{C_{nominal}}{n} \quad (27)$$

4.2.2. Control Algorithm for BESS

One of the most flexible methods for the superior performance of BESS in DC grid is to connect the battery by a proper DC/DC converter. A bi-directional Buck-Boost DC/DC converter shown in Fig. 11 is used in the current study. Under different micro-grid conditions, the BESS operates at charging, discharging or floating modes and the modes are managed according to the DC bus voltage condition at the point of BESS coupling. Consequently, the BESS is required to provide necessary DC voltage control under different operating modes of the micro-grid regarding the relatively large time constant of the battery, it can be modeled as a constant voltage source in small signal analysis. The average state-space model of the battery converter could be defined by the following equations. Regarding the relatively large time constant of the battery, it can be modeled as a constant voltage source in small signal analysis. The average state-space model of the battery converter could be defined by the following equations.

$$\frac{di_{batt}}{dt} = \left(\frac{1-d}{L}\right) vo + \frac{Rl}{L} i_{batt} + \frac{d}{L} V_{batt} \quad (28)$$

$$\frac{dv_{Co}}{dt} = (\frac{1-d}{Co}) i_{batt} - \frac{1}{Co} i_o v_o = R_o C_o \frac{dvo}{dt} + v_{Co} \quad (29)$$

The control-to-output transfer function of the converter can be expressed by

$$\frac{\hat{v_o}}{d} = \frac{Vo(1-D)}{LCo} \frac{(1+C_o R_o S}{S^2 + \frac{C_o(R_L+(1-D^2)R_o)}{LC_o} S + \frac{(1-D)^2}{LC_o}} \quad (30)$$

4.3. Grid Side VSC Control Method

As discussed earlier, the function of GS-VSC is to regulate the DC-link voltage during grid connected mode. A two level VSC is used to link DC and AC grids. Peak current-mode control approach [2] is exploited for real/reactive power control at AC side. Thus, the amplitude and the phase angle of the VSC terminal voltage are controlled in a d q rotating reference frame. The DC-link voltage control is accomplished through the control of the real power component. DC voltage dynamics can be formulated based on the principle of power balance, as:

$$\frac{d}{dt}(\tfrac{1}{2}C.VDC^2) = P_{dc} - P_{ac} \quad (30)$$

$$P_{dc} = V_{DC}.i_{grid}^{DC} \quad (31)$$

Table 1. *Rating of the DC micro-grid elements.*

DC micro- grid	Nominal voltage	400 V
Transformer	Nominal voltage	600/240 V
Total DC load	constant power	11KW
Wind turbine	Rate power	50KVA
	Rate Voltage	480V
	Frequency	50Hz
	Stator resistance	0.00706 PU
	Stator reactance	0.171 PU
	Rotor *resistance*	0.005 PU
	Rotor reactance	0.156 PU
	Pole	6
PV system	Rate power	15KW
	Rate Voltage	500V
	Short circuit current	25.44A
	Short circuit voltage	66V
	The temperature	$0-1400^o$
	The number of panels	24
	R, L, C, Co	1Ω, 0.01H, 2mF, 2mF
BESS	Type	Lithium-ion
	Rate power	30KW
	Rate Voltage	500V
	Rating	65Ah
	Battery converter	2500Hz

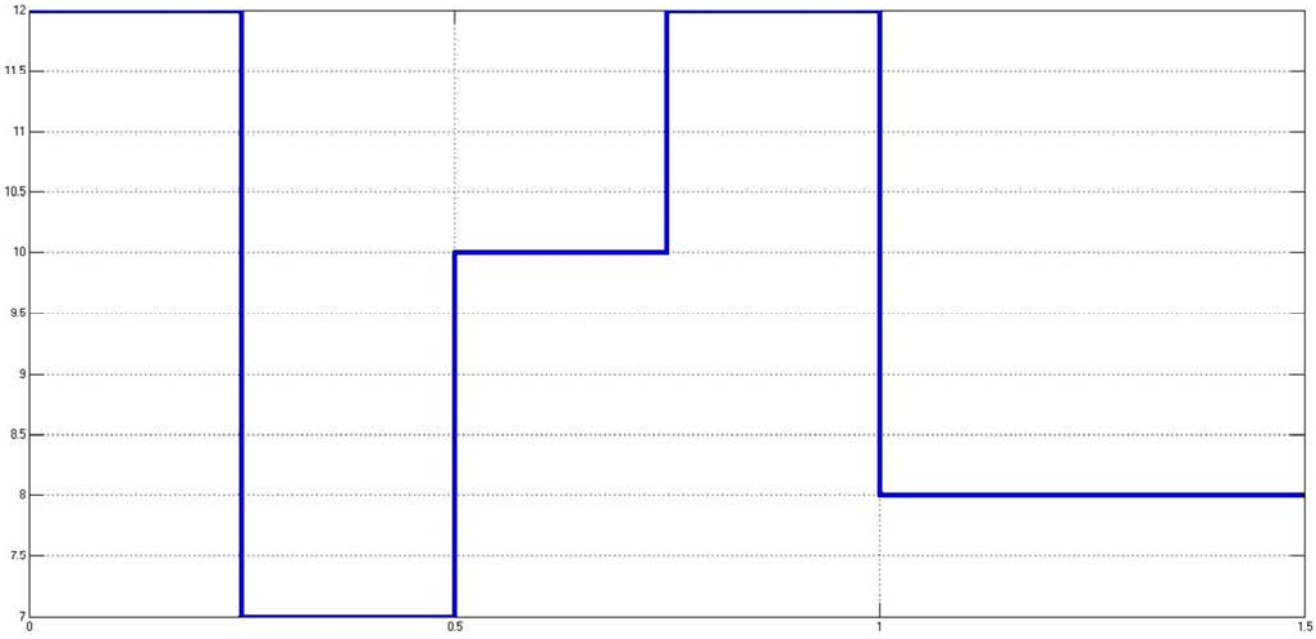

Figure 9. *Input wind speed variation.*

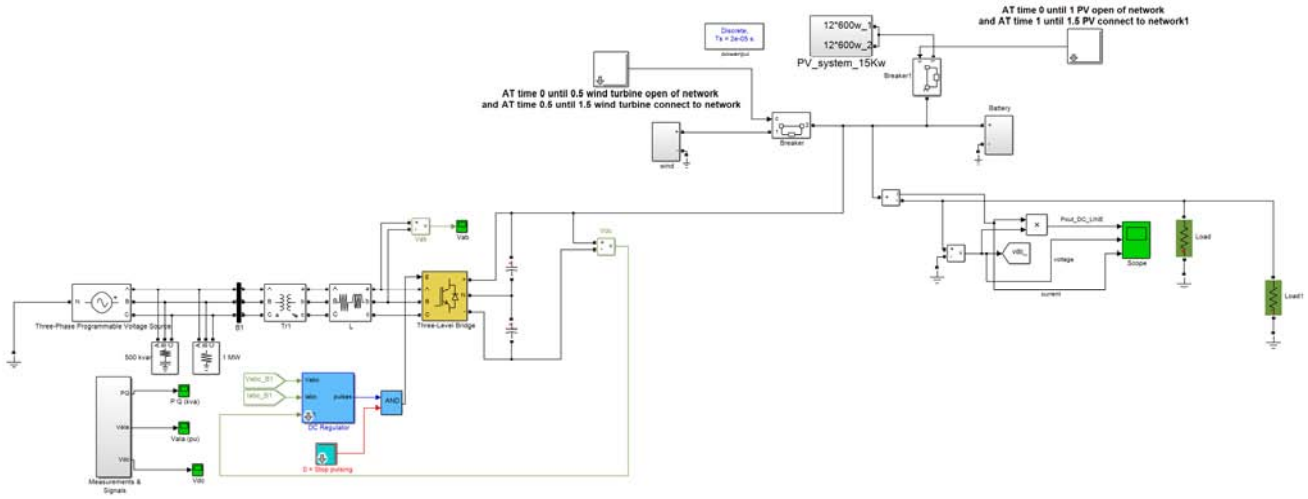

Figure 10. *The simulated DC micro-grid.*

5. Simulation Results

Mode. 4. 1 Micro - grid DC converter mode network connectivity (Grid): micro- grid DC in various situations against the sudden tensions in or out of any of these resources has been studied in which both wind turbine and photovoltaic systems were connected to the grid for 0.5 and 1 sec respectively the results have been shown in the figure below:

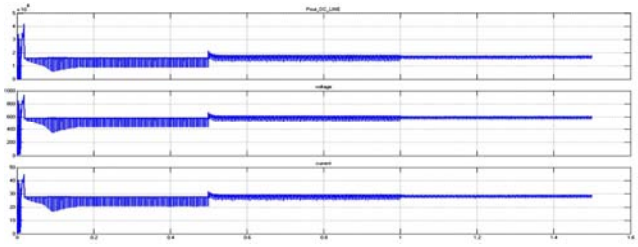

Figure 11. *Power and voltage and DC current to the load.*

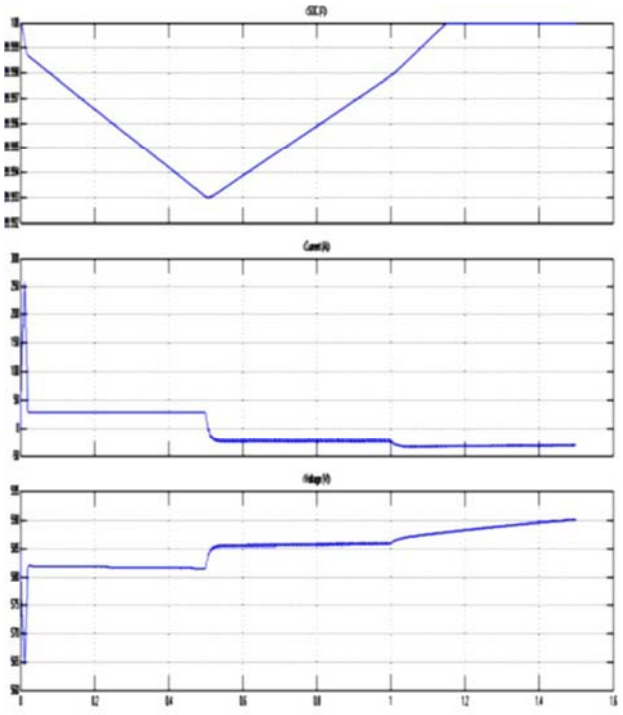

Time (s)

Figure 12. *SOC, battery voltage and current.*

Mode 4.2 DC micro-grid including wind turbine, photovoltaic systems and battery storage will be connected to grid at the 1.1sec.

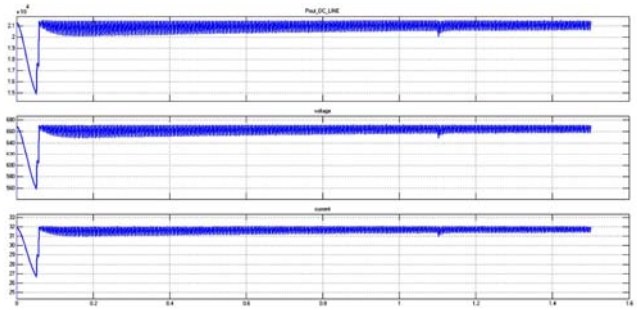

Time (s)

Figure 13. *Power and voltage and DC current to the load.*

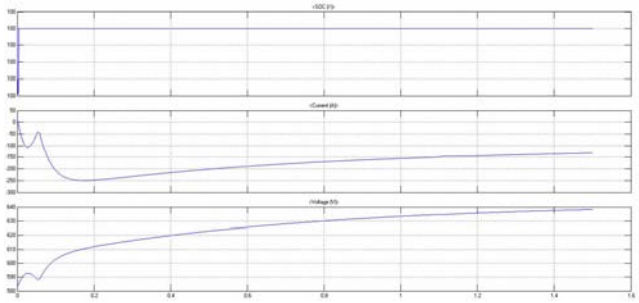

Time (s)

Figure 14. *SOC, battery voltage and current.*

Mode 4.3 micro-grid DC, Island mode:

Mode 4.3.1. In this mode battery storage system will be connected to the micro-grid permanently and as in mode 4.2 which mentioned above again wind turbine and photovoltaic systems being connected to micro-grid as island.

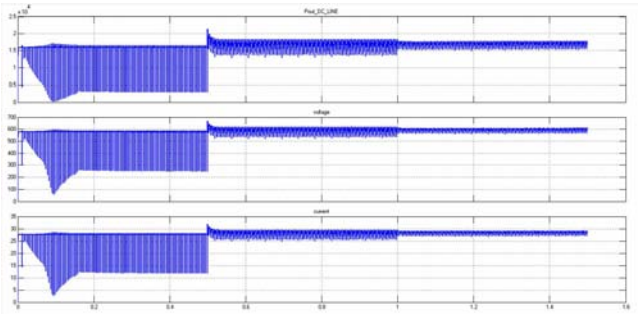

Time (s)

Figure 15. *Power and voltage and DC current to the load.*

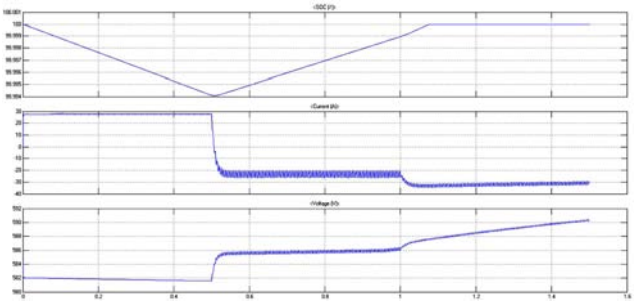

Time (s)

Figure 16. *SOC battery voltage and current.*

Mode4.3.2 the battery storage system will be excluded from the micro-grid system permanently then both wind turbine and photovoltaic systems will be connected to micro-grid at 0.5 & 1 sec s respectively.

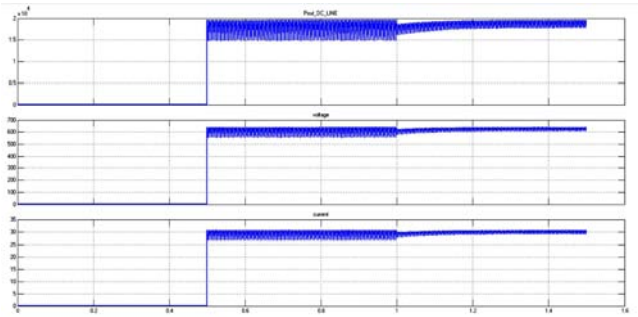

Time (s)

Figure 17. *Power and voltage and DC current to the load.*

Mode4.4 in this mode battery reconnected to the micro-grid at 1.1 sec, but this time wind turbine will be bypassed from the micro-grid at 0.5 sec and at the same time photovoltaic system being connected to micro-grid.

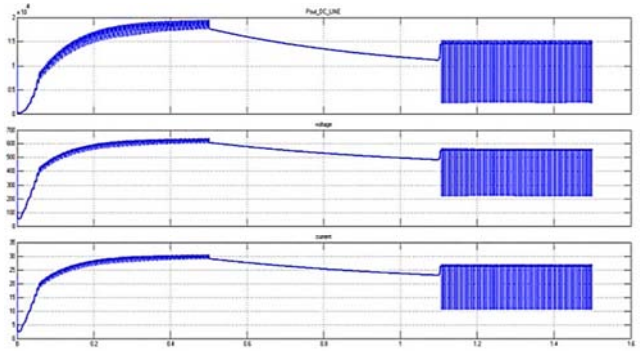

Time (s)

Figure 18. *Power and voltage and DC current to the load.*

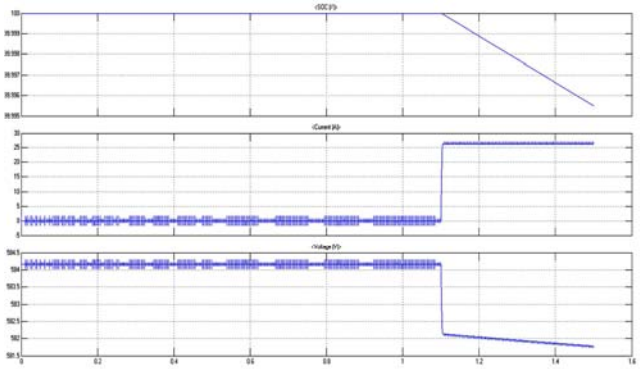

Time (s)

Figure 19. *SOC battery voltage and current.*

Mode.4.5 in this mode battery system again bypassed and wind turbine connected to the micro-grid from the beginning, wind speed changes being shown in figure 12, then photovoltaic system being connected to micro-grid at 0.5 sec and changes of sun light rate, change rate between 800 to 1100 considered for 24 panels (6 panels 1100, 6 panels 1000, 6 panels 900 and 6 panels 800) all in Island form.

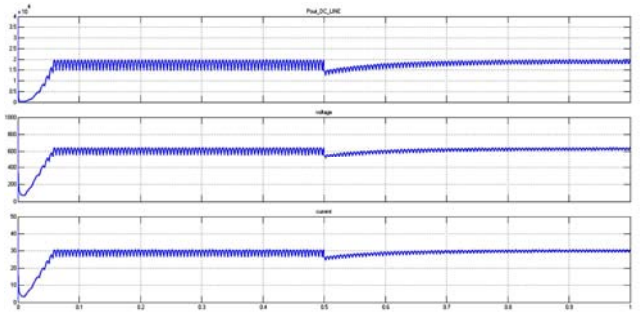

Time (s)

Figure 20. *Power and voltage and DC current to the load.*

Mode.4.6 in this mode battery system will be connected to the micro-grid from the start, photovoltaic and wind speed changes are similar to mode 4.5, then at 0.5 sec load changes equal to 10kw will be applied to the micro-grid system which leads to 20 kw extra load, as a result 20 kw load separated from micro-grid at 1sec.

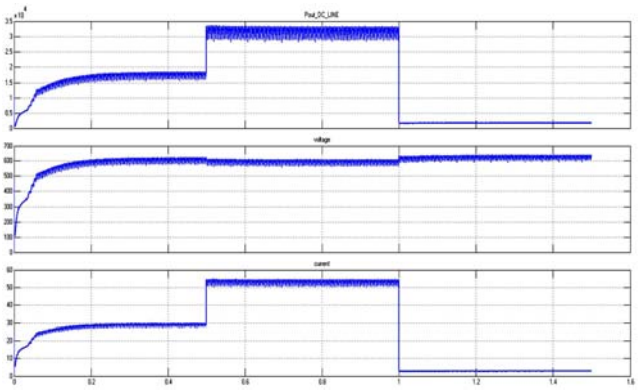

Time (s)

Figure 21. *Power and voltage and DC current to the load.*

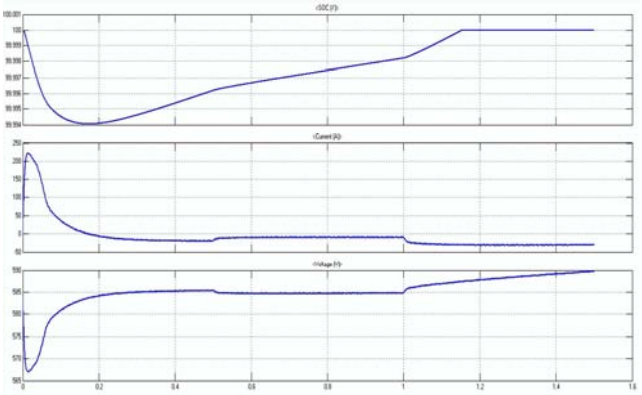

Time (s)

Figure 22. *SOC, battery voltage and current.*

6. Conclusion

This paper proposes a Control strategy for distributed integration of photovoltaic and energy storage and wind power systems in DC micro-grid including variable loads and solar radiation. The requirement of maintaining constant DC voltage is realized, considering different operating modes in grid connected and islanded states the proposed control enables the maximum utilization of PV power during different operating conditions of the micro-grid and provides a smooth transfer between the grid connection and islanded mode. DC voltage levels are used as a communication link in order to coordinate the sources and storages in the system and acts as a control input for the operating mode switching during different operation conditions. When the system is network - independent, and the exploitation of natural and production of active power by a converter AC balance will be funded constant DC voltage is guaranteed. System simulations have been carried out in order to validate the proposed control methods for the distributed integration of PV and energy storage and wind power in a DC micro-grid and the results show the reasonable operation of the micro-grid during various disturbances.

References

[1] K. Manohar, "Mppt and Simulation for a Grid-Connected Photovoltaic System and Fault Analysis" IJES, vol 1, 2, 2012.

[2] *Hamed Babazadeh, Wenzhong Gao, Kurtis Duncan, "A New Control Scheme in a Battery Energy Storage System for Wind Turbine Generators," IEEE, vol 978, 7, 2012.*

[3] Ji-Heon Lee, "DC Micro-Grid Operational Analysis with a Detailed Simulation Model for Distributed Generation," JPE, 2011.

[4] K. R. Padiyar and P. Nagesh, "Design and performance evaluation of subsynchronous damping controller with STATCOM," Power Delivery, IEEE Transactions on, vol. 21, no. 3, pp. 1398–1405, 2006.

[5] S. Purushothaman and F. de León, "Eliminating Subsynchronous Oscillations With an Induction Machine Damping Unit (IMDU)," Power Systems, IEEE Transactions on, vol. 26, no. 1, pp. 225–232, 2011.

[6] T. Porselvi, Ranganath Muthu, "Design of Buck-Boost Converter for Wind Energy Conversion System," European Journal of Scientific Research, vol 83, 11, 2012.

[7] S. O. Faried, I. Unal, D. Rai, and J. Mahseredjian, "Utilizing DFIG-Based Wind Farms for Damping Subsynchronous Resonance in Nearby Turbine-Generators," IEEE TRANSACTIONS ON POWER SYSTEMS, vol. 28, no. 1, pp. 452 – 459, 2013.

[8] T. Aziz, K. Saha, N. Mithulananthan, "Analysis and Mitigation of Transient Over voltage with Integration of Small Scale Power-Electronic Interfaced DG," IEEE, vol 9, 8, 2012.

[9] Lihui Yang, Zhao Xu, Zhao Yang Dong, Kit Po Wong, "Advanced Control Strategy of DFIG Wind Turbines for Power System Fault Ride Through," IEEE, vol 27, 10, 2012.

[10] Metin Kesler, Engin Ozdemir, "Synchronous-Reference-Frame-Based Control Method for UPQC Under Unbalanced and Distorted Load Conditions," IEEE, vol 58, 9, 2011.

[11] Ramadoni syahputra, Mochamad ashari, Imam robandi, "Modeling and Simulation of Wind Energy Conversion System in Distributed Generation Units, Proceedings of International Seminar on Applied Technology, " Science and Arts, 7, 2011.

[12] Savita Nema, R. K. Nema, Gayatri Agnihotri, "Matlab / simulink based study of photovoltaiccells / modules / array and their experimental verification," IJEE, vol1, 14, 2010.

[13] Zhou Yunhai, Jürgen Stenzel, "Simulation of a Microturbine Generation System for Grid Connected and Islanding Operations," IEEE, 5, 2009.

[14] A. Ch. Kyritsis, E. C. Tatakis, and N. P. Papanikolaou, "Optimum Design of the Current Source Flyback Inverter for Decentralized Grid-Connected Photovoltaic Systems,"IEEE, vol 23, 13, 2008.

[15] D. Rai, F. Sherif, R. Gokaraju, and E. A.-A. A, "An SSSC-Based Hybrid Series Compensation Scheme Capable of Damping Subsynchronous Resonance," Power Delivery, IEEE Transactions on, vol. 27, no. 2, pp. 531–540, 2012.

[16] Tsai-Fu Wu, Hung-Shou Nien, Hui-Ming Hsieh, and Chih-Lung Shen, "PV Power Injection and Active Power Filtering With Amplitude-Clamping and Amplitude-Scaling Algorithms, "IEEE, vol 43, 11, 2007.

[17] Yi Huang, Miaosen Shen, "Z-Source Inverter for Residential Photovoltaic Systems," IEEE, vol 21, 7, 2006.

[18] Weidong Xiao, Magnus G. J. Lind, William G. Dunford, "Real-Time Identification of Optimal Operating Points in Photovoltaic Power Systems,"IEEE, vol 53, 10, 2006.

[19] E. Bhasker, M. Kiran Kumar, "Three-Phase Five-Level PWM DC–DC Con Using H-Bridge," International Journal of Modern Engineering Research, 2, 5, 2012.